IOPscience iopscience.iop.org

Home Search Collections Journals About Contact us My IOPscience

Vapour spreading and the boiling crisis

This article has been downloaded from IOPscience. Please scroll down to see the full text article.

2003 J. Phys.: Condens. Matter 15 S435

(http://iopscience.iop.org/0953-8984/15/1/360)

View the table of contents for this issue, or go to the journal homepage for more

Download details:
IP Address: 171.66.16.119
The article was downloaded on 19/05/2010 at 06:25

Please note that terms and conditions apply.

INSTITUTE OF PHYSICS PUBLISHING JOURNAL OF PHYSICS: CONDENSED MATTER

J. Phys.: Condens. Matter **15** (2003) S435–S442 PII: S0953-8984(03)55077-9

Vapour spreading and the boiling crisis

D Beysens[1,2,3], V Nikolayev[1] and Y Garrabos[2]

[1] ESEME, Service des Basses Températures, DSM/DRFMC, CEA-Grenoble, France
[2] CNRS-ESEME, Institut de Chimie de la Matière Condensée de Bordeaux,
87, Avenue du Dr Schweitzer, 33608 Pessac Cedex, France

E-mail: dbeysens@cea.fr

Received 22 October 2002
Published 16 December 2002
Online at stacks.iop.org/JPhysCM/15/S435

Abstract

The boiling crisis (BC) is well known in the world of heat and mass transfer. It is a transition from nucleate boiling (i.e. boiling in its usual sense) to film boiling, where the heater is covered by a continuous vapour film. The BC is observed when the heat flux from the heater exceeds a critical value. Heat exchange then falls down and endangers the exchanger whose temperature rises abruptly. The physical mechanism of the BC is still under debate. We propose the recoil force (the thrust of vapour production) at the solid–liquid–vapour contact line to lie at the origin of the BC. At large heat flux, the recoil force tends to spread the vapour bubble that otherwise would not wet the solid. We give both analytical and numerical analysis in support of this idea. We also report experiments under microgravity conditions performed with near-critical fluids (SF_6 and CO_2). The absence of gravity effects and the vicinity of the critical point where the liquid–vapour surface tension vanishes emphasize the influence of the recoil force: during heating, the vapour drop is indeed seen to spread.

1. Introduction

Boiling is a very efficient way to transfer heat from solid to liquid. The bubble growth in boiling has attracted much attention from many scientists and engineers. In spite of these efforts, some important aspects of the growth of a vapour bubble attached to a solid heater remain misunderstood even on a phenomenological level. The most important aspect is the 'boiling crisis' (BC), a transition from nucleate boiling (where vapour bubbles nucleate on the heater) to film boiling (where the heater is covered by a continuous vapour film). The BC is observed when the heat flux q_S from the solid heater exceeds a threshold value which is called the 'critical heat flux' (CHF). The rapid formation of the vapour film on the heater surface

[3] Author to whom any correspondence should be addressed. Mailing address: CNRS-ESEME, Institut de Chimie de la Matière Condensée de Bordeaux, 87, Avenue du Dr Schweitzer, 33608 Pessac Cedex, France.

 © 2003 IOP Publishing Ltd Printed in the UK

decreases the heat transfer steeply and leads to a local heater overheating. In the industrial heat exchangers, the BC can lead to melting of the heater, thus leading to a potentially dangerous accident. Therefore, the determination of the CHF is extremely important.

A clear understanding of the triggering mechanism of the BC is still lacking. The knowledge of what happens at the foot of the bubble which grows attached to the heater is crucial for the correct modelling of the BC. We proposed recently [1] that the recoil force (the thrust of production of vapour), by making the bubble spread over the heater surface, could lie at the origin of the BC. Numerical simulations of the thermal field around the bubble [2] support this claim.

The experimental observations at large heat fluxes close to the CHF are complicated by the violence of boiling and optical distortions caused by the strong temperature gradients. Nevertheless, near the critical point, the CHF is very small and the bubble evolution is very slow. We recently carried out boiling experiments under microgravity in the proximity of the critical point [3]. Microgravity, which cancels buoyancy forces, is a powerful tool for studying the phenomena near the vapour–liquid–solid contact line. In the present report we review the main results obtained theoretically and compare with the microgravity experiments.

2. The recoil force at the triple contact line

BC is a really universal phenomenon which occurs inevitably for pool boiling as well as for flow boiling and for different flow structures, flow velocities, and liquid temperatures and pressures. The phenomenon is local [4]: it depends strongly only on the local values of the parameters in a very thin layer of liquid adjacent to the heating surface. The most important parameter is the distribution of the local temperature. As a consequence of the local origin of the BC, the threshold depends strongly on the wetting properties of the heating surface. Numerous experiments [5, 6] show the general tendency: a poor wetting of the heating surface by the liquid decreases the CHF and vice versa.

Experiments on visualization [7, 8] of dry spots under the vapour bubbles on the heating surface show that at the CHF a *single* dry spot suddenly begins to spread. In [9–11] the vapour recoil instability [12] is proposed as a reason for the BC. Although it is not clear how an instability can induce the spreading of the dry spots, the authors show that the vapour recoil force can be important at large evaporation rates. The force originates in the uncompensated momentum of vapour which is generated on the liquid–vapour interface during the evaporation. In the reference frame of the bulk liquid, the momentum conservation implies

$$\vec{P}_r + \eta(\vec{v}_V + \vec{v}_i) = 0, \tag{1}$$

where $\vec{P}_r$ is the vapour recoil force per unit interface area, η is the evaporated mass per unit time and unit interface area, $\vec{v}_i$ is the interface velocity, and $\vec{v}_V$ is the vapour velocity with respect to the interface. It is easy to establish that $\vec{v}_i = -(\eta/\rho_L)\vec{n}$, where $\vec{n}$ is a unit vector normal to the interface directed inside the vapour bubble (figure 1). The mass conservation on the interface yields $\vec{v}_V = -(\rho_L/\rho_V)\vec{v}_i$, where ρ_L and ρ_V are the mass densities of the liquid and the vapour. Therefore, equation (1) implies [12]

$$\vec{P}_r = -\eta^2(\rho_V^{-1} - \rho_L^{-1})\vec{n}. \tag{2}$$

The surface deformation caused by this force is important whenever the evaporation is strong.

The rate of evaporation η can be related to the local heat flux across the interface q_L by the equality

$$q_L = H\eta, \tag{3}$$

where H is the latent heat of evaporation. Hereafter, we neglect heat conduction in the vapour with respect to the latent heat effect.

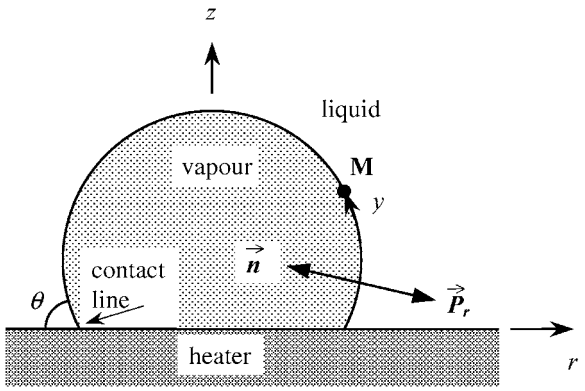

Figure 1. A vapour bubble on the heating surface surrounded by liquid. The directions of the vectors $\vec{P}_r$ and $\vec{n}$ are shown as well as the axes for the coordinate system.

3. Vapour recoil and bubble spreading

Below, we consider a case of a system at high pressure, where the growth of the bubble is slow and the problem may be considered in the quasi-static approximation.

The spreading of the dry spot looks similar to the spreading of a liquid that wets a solid. But in the case of the BC, it is *vapour* that spreads over the solid. This never happens for a non-metal liquid under equilibrium conditions (zero heat flux) on a perfectly clean and smooth metal surface [14], the finite contact angle being possible due to the surface defects only. A kind of drying transition occurs due to the vapour recoil force at some heat flux that we associate with the CHF.

Using the quasi-static approximation, the variational approach [15] can be applied to analyse the shape of a vapour bubble just before the BC. The free energy of the system consists of two parts. The first part is conventional [15]:

$$U_1 = \sigma A + \sigma_{VS} A_{VS} + \sigma_{LS} A_{LS} - \lambda V, \tag{4}$$

where σ, σ_{VS}, and σ_{LS} are the surface tensions for vapour–liquid, vapour–solid, and liquid–solid interfaces respectively; A_{VS} and A_{LS} are the corresponding interface areas; and A is the area of the vapour–liquid interface. The last term in (4) reflects the fact that the shape of the bubble should be found for its given volume V, λ (i.e. the Lagrange multiplier) being the difference between the pressures inside and outside of the bubble.

The second part U_2 of the free energy accounts for the virtual work of the external forces:

$$\delta U_2 = -\int_{(A)} \vec{P}_r \cdot \delta\vec{r}\, \mathrm{d}A. \tag{5}$$

The minimization $\delta U_1 + \delta U_2 = 0$ of the total energy leads [15] to two equations. The first is the condition for local equilibrium of the interface:

$$K\sigma = \lambda + P_r, \tag{6}$$

where K is the local curvature of the bubble and $P_r = |\vec{P}_r|$. The second equation is $\cos\theta = b$, where $b = (\sigma_{VS} - \sigma_{LS})/\sigma$ and θ is the contact angle (figure 1). For the case $b > 1$ the second equation should be replaced by the condition $\theta = 0$.

Let us denote by y the distance along the bubble contour measured from the triple line to a given point M as shown in figure 1. To find the bubble shape by solving equation (6) we need to know the vapour recoil as a function of y. In the following, we introduce a

rough approximation to solve the very complicated problem of the heat exchange around the growing bubble. The case of saturated boiling is assumed. Thus the vapour–liquid interface is maintained at temperature T_s, the saturation temperature at the system pressure. We also assume for simplicity that the thermal effect of convection can be taken into account by renormalizing the liquid thermal conductivity. To estimate how P_r varies near the contact line (i.e. when $y \to 0$) we suppose the bubble to be two dimensional with the contact angle $\theta = \pi/2$. Since we describe the heat exchange in a thin layer adjacent to the heating surface, we can imagine the bubble contour A to be a line Oy perpendicular to the Ox heater line. Then q_L can be obtained from the solution of a simple two-dimensional problem of unsteady heat conduction in a quarter plane $x, y > 0$, the point O($x = 0, y = 0$) corresponding to the contact line. The boundary and the initial conditions for this problem can be written in the form $T_L|_{x=0} = T_s$, $-k_L\,\partial T_L/\partial y|_{y=0} = q_S$, $T_L|_{t=0} = T_s$, where $T_L(x, y, t)$ is the liquid temperature, k_L is the liquid thermal conductivity, and q_S is the heat flux from the heating surface which is assumed to be uniform for the case of the thin heating wall. The solution for this problem of heat conduction reads

$$T_L = T_s + \frac{q_S}{k_L}\sqrt{\frac{\alpha_L}{\pi}}\int_0^t \frac{\mathrm{d}t}{\sqrt{t}}\,\mathrm{erf}\left(\frac{x}{2\sqrt{\alpha_L t}}\right)\exp\left(-\frac{y^2}{4\alpha_L t}\right), \tag{7}$$

where α_L is the liquid thermal diffusivity. This solution implies the following expression for $q_L(y)$:

$$q_L = -k_L\frac{\partial T_L}{\partial x}\bigg|_{x=0} = -\frac{q_S}{\pi}E_1\left(\frac{y^2}{4\alpha_L t}\right). \tag{8}$$

The exponential integral $E_1(y)$ [16] decreases as $\exp(-y)/y$ as $y \to \infty$ and diverges logarithmically at the point $y = 0$. In the following we will use for illustration the dependence $P_r(y)$ in the form that retains these physical features:

$$P_r = -C\log(y/L)\exp[-(y/y_r)^2], \tag{9}$$

where L is the length of the half-contour of the 3D axially symmetrical bubble and C is a constant. The characteristic length of the vapour recoil decay y_r changes over time and is proportional to $\sqrt{\alpha_L t}$ (cf (8)). Meanwhile, the bubble grows and its radius is proportional to the same factor [13] during the late stages of its growth. Therefore, y_r is proportional to the bubble size, this fact is taken care of by the expression

$$y_r = aL, \tag{10}$$

where a is the non-dimensional fraction of the bubble surface on which the vapour recoil is important. From the physical point of view, y_r characterizes the width of the superheated layer of liquid, which is always less than the bubble size [13]; thus $a \ll 1$. This allows the upper limit of integration to be put to infinity in the following expression for the non-dimensional strength of the vapour recoil:

$$N_r = \frac{1}{\sigma}\int_0^\infty P_r\,\mathrm{d}y. \tag{11}$$

The integration can be performed analytically, yielding the relation between C and N_r: $N_r = [CaL/(4\sigma)]\sqrt{\pi}[\gamma + \log(4/a^2)]$, where $\gamma = 0.577\ldots$ is Euler's number [16]. Although the expression (9) for the vapour recoil pressure is not rigorous, it contains the main physical features of the solution of the heat conduction problem: a weak divergence at the contact line and a rapid decay away from it. It is shown in [2] that the rigorous numerical solution obtained far from the critical point follows this behaviour.

At low pressures, when the bubble growth is fast, additional ('inertial resistance') forces of hydrodynamic origin should be included into (6). In addition, the influence of the associated

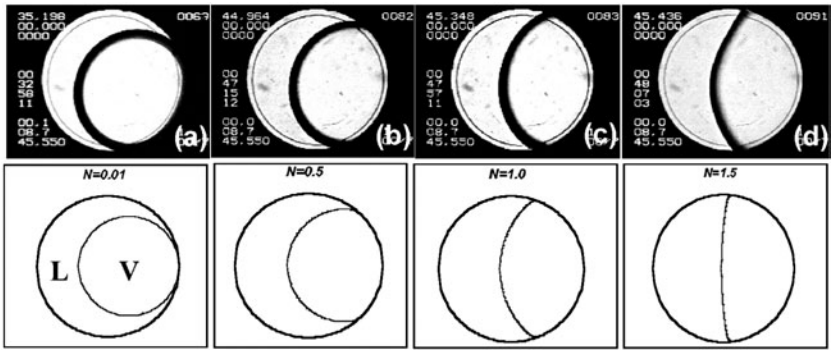

Figure 2. (a)–(d) A time sequence of cell images during a temperature ramp. The calculated bubble shape for different values of the non-dimensional strength of vapour recoil N_r that goes to infinity at the critical point is shown in the lower row. Note that the actual contact angle is zero for all the curves.

convection on the temperature variation should be taken into account. However, the vapour recoil should still control the bubble spreading.

4. Experiments under microgravity near a critical point

We consider here results that were obtained using a sample of SF_6 at near-critical density (off by +0.25%). The critical coordinates of SF_6 are: $T_c = 318.717$ K, $\rho_c = 742$ kg m^{-3}, $p_c = 3.754$ MPa. The sample was heated at various rates in a cylindrical cell on the Mir space station using the Alice-II instrument [18]. This instrument is specially designed to obtain high-precision temperature control (stability of $\approx$15 μK over 50 h, repeatability of $\approx$50 μK over seven days). To place the sample near the critical point, a constant-mass cell was prepared with a high-precision density, to 0.02%, by observing the volume fraction change of the cells as a function of temperature on the ground. The fluid layer is sandwiched between two parallel sapphire windows and surrounded by a copper alloy housing in the cylindrical optical cell with an inner diameter of 12 mm and the thickness $H = 1.664$ mm.

The liquid–gas interface is visualized through light transmission normal to the windows. Since the windows were glued to the copper alloy wall, some of the glue is squeezed inside the cell. This glue forms a ring that blocks the light transmission in a thin layer of the fluid adjacent to the copper wall making it inaccessible for observations. Because of this glue layer, the windows may also be slightly tilted with respect to each other. As the drop is pressed against the windows, even a tiny angle between them results in a steady force that pushes the bubble toward the wall; see figure 2. A 10 mm diameter ring was engraved on one of the windows of each cell in order to calibrate the size of the images. The sample cell is placed inside a thermostat. The temperature is sampled every second and is resolved to 1 μK.

The cell is heated from room temperature nearly linearly in time t at a rate $\approx$7.2 mK s^{-1}. Figure 2 shows the time sequence of the images of the cell. The interface appears dark because the liquid–gas meniscus refracts the normally incident light away from the cell axis. After the temperature ramp is started but still far from the critical temperature, the bubble shape changes. The contact area A_{VS} of the gas with the copper wall appears to increase. This increase is accompanied by an evident increase in the apparent contact angle; see figure 2.

Temperature quenches—i.e. fast temperature jumps from one temperature to another—were also performed, at different distances from T_c. The typical value for a quench is 0.1 K. The

quench images [3] also show bubble spreading, slight far from the critical point and stronger near the critical point. After each quench, as soon as the heating stops, the bubble interface begins to return to its initial form.

5. Interface evolution during heating

The above experimental data showed that the spreading gas and the associated interface deformation are caused by an out-of-equilibrium phenomenon. Marangoni convection due to a temperature change δT_i along the gas–liquid interface cannot be the source of such an evolution, since (i) convection is not observed in the video films and (ii) the interface must remain at constant (saturation) temperature throughout the process [3].

The bubble is thus deformed by the normal stress exerted on the interface by the recoil from departing vapour. The interface shape can be determined from (6), where the 3D curvature K is equal to the sum of the 2D curvature c in the image plane and the 2D curvature in the perpendicular plane. For the small cell thickness H, this latter curvature can be accurately approximated by the constant value $2/H$. This is possible because the relatively small heat flow through the less conductive sapphire windows implies a small P_r near the contact line on the windows, as compared to the large value of λ for this small H. The interface shape can thus be obtained from the 2D equation

$$\sigma c = \lambda' + P_r(y), \tag{12}$$

where λ' is a constant to be determined from the known vapour area at the image and y is a coordinate that varies along the bubble contour in the image plane as in figure 1.

In order to find the distribution of the evaporation rate $\eta(\vec{x})$ at the interface it is necessary to solve the entire heat transfer problem. Because the bulk temperature varies sharply in the boundary layer adjacent to the walls of the cell and the interface temperature is constant, the largest portion of mass transfer across the interface takes place near the triple contact line. Thus $\eta(\vec{x})$ is large in the vicinity of the contact line.

We assume that $\eta(\vec{x})$ has the following form:

$$\eta(\vec{x}) = g(\vec{x})(T_c - T)^{\omega} \tag{13}$$

as $T \to T_c$, i.e., it has the same local behaviour with respect to temperature as the critical temperature is approached. The integral rate of change of mass M of the gas bubble is defined as

$$\mathrm{d}M/\mathrm{d}t = \int \eta(\vec{x})\,\mathrm{d}\vec{x} \sim (T_c - T)^{\omega}, \tag{14}$$

where the integration is performed over the total gas–liquid interface area. On the other hand,

$$\mathrm{d}M/\mathrm{d}t = \mathrm{d}(V\phi\rho_G)/\mathrm{d}t, \tag{15}$$

where $\phi = 0.5$ is the gas volume fraction. Near the critical point, the coexistence curve has the form $\rho_G = \rho_c - \Delta\rho/2$, where $\Delta\rho \sim (T_c - T)^{\beta}$ with the universal exponent $\beta = 0.325$, so $\mathrm{d}M/\mathrm{d}t \sim (T_c - T)^{\beta-1}(\mathrm{d}T/\mathrm{d}t)$ as $T \to T_c$ according to equation (15). Thus equation (14) results in $\omega = \beta - 1$ and the curvature change due to the vapour recoil scales as

$$P_r/\sigma \sim (T_c - T)^{3\beta-2-2\nu}, \tag{16}$$

where equation (2) and the scaling relationship $\sigma \sim (T_c - T)^{2\nu}$ ($\nu = 0.63$) were employed. Because this critical exponent ($3\beta - 2 - 2\nu \approx -2.3$) is very large, it manifests itself even far from the critical point in agreement with the experiments. In summary, as $T \to T_c$, the vapour mass growth follows the growth of its density (the vapour volume remains constant), so the diverging vapour production near the critical point drives a diverging recoil force.

This curvature change has a striking effect on the bubble shape because it is not homogeneously distributed along the bubble interface. Since the evaporation is strongest near the copper heating wall where the strongest temperature gradients form, both P_r and c increase strongly near this wall, i.e. near the triple contact line. Because the interface slope changes so abruptly near the contact line, the apparent contact angle is much larger than its actual value.

In order to illustrate a possible solution of equation (12), we solved it for $P_r(y)$ as above in equation (9) with $y_r = 0.1L$, following the method described in [1]. The result of this calculation is shown in figure 2. Since equation (16) implies

$$N_r \sim (T_c - T)^{-2.3} \to \infty \tag{17}$$

as $T \to T_c$, the increase in N_r mimics the approach to the critical point and qualitatively explains the observed shape of the vapour bubble (see figure 2). The increase of the apparent contact angle and of the gas–solid contact area A_{VS} can be seen in this figure 2.

6. Conclusions

Very similar bubble spreadings are also observed far from T_c (i.e. at low pressures) during boiling at large heat flux [7, 8]. The main difference is that the large value of N_r results from a large vapour production that can be achieved during strong overheating rather than from the critical effects. Although we did not model this case characterized by the influence of 'inertial resistance' hydrodynamic forces that distort the bubble, the vapour spreading due to vapour recoil still exists. The vapour recoil mechanism is thus a quite general explanation for the BC.

It is well documented from experiments [13] that the CHF decreases rapidly when the fluid pressure p approaches the critical pressure p_c, i.e., when $T \to T_c$ in our constant-volume system. Previously, this tendency has not been well understood. The divergence of the factor N_r, discussed above, helps us to understand it. We first note that the evaporation rate η scales as the applied heat flux q_S and $N_r \sim q_S^2$, where equations (2) and (11) are used. By assuming that the BC ($q_S = q_{CHF}$) begins when N_r attains its critical value $N_{CHF} \sim 1$ (i.e. when the vapour bubbles begin to spread), one finds that

$$q_{CHF} \sim (T_c - T)^{1+\nu-3\beta/2} \sim (T_c - T)^{1.1} \tag{18}$$

from equation (17). The same exponent is also valid for the pressure scaling:

$$q_{CHF} \sim (p_c - p)^{1.1}. \tag{19}$$

Equation (19) explains the observed tendency $q_{CHF} \to 0$ as $p \to p_c$.

Although the strict requirements on temperature stability and the necessity of weightlessness lead to experimental difficulties for studying the BC in the near-critical region, they also present some important advantages. Only a very small heating rate (heat flux) is needed to reach the BC because q_{CHF} is very small. At such low heat fluxes, the bubble growth is extremely slow due to the critical slowing down. In our experiments, we were able to observe the spreading gas (i.e. the dry-out that leads to the BC; see figure 2) for 45 min. Such experiments not only permit an excellent time resolution, but also allow the complicating effects of rapid fluid motion to be avoided.

Acknowledgments

We thank our colleagues J Hegseth and C Lecoutre for help and fruitful discussions.

References

[1] Nikolayev V S and Beysens D A 1999 *Europhys. Lett.* **47** 345–51
[2] Nikolayev V S, Beysens D A, Lagier G-L and Hegseth J 2001 *Int. J. Heat Mass Transfer* **44** 3499–511
[3] Garrabos Y, Lecoutre-Chabot C, Hegseth J, Nikolayev V S and Beysens D 2001 *Phys. Rev.* E **64** 051602-1–10
[4] Bricard P, Péturaud P and Delhaye J-M 1997 *Multiphase Sci. Technol.* **9** 329–79
[5] Katto Y 1994 *Int. J. Multiphase Flow* **20** 53
[6] Diesselhorst T, Grigull U and Hahne E 1977 *Heat Transfer in Boiling* ed E Hahne and U Grigull (New York: Hemisphere) p 99
[7] van Ouwerkerk H J 1972 *Int. J. Heat Mass Transfer* **15** 25
[8] Torikai K, Suzuki K and Yamaguchi M 1991 *JSME Int. J. Ser. II* **34** 195
[9] Sefiane K, Benielli D and Steinchen A 1998 *Colloids Surf.* **142** 361
[10] Pavlov P A and Liptchak A I 1992 *Metastable Phase States and Kinetics of Relaxation* (Sverdlovsk: Russian Academy of Sciences, Ural Division) p 119 (in Russian)
[11] Avksentyuk B P and Ovchinnikov V V 1995 *Two-Phase Flow Modelling and Experimentation* ed G P Celata and R K Shah (Pisa: Edizioni ETS) p 1205
[12] Palmer H J 1976 *J. Fluid Mech.* **75** 487
[13] Tong L S 1997 *Boiling Heat Transfer and Two-Phase Flow* 2nd edn (New York: Taylor and Francis)
[14] de Gennes P G 1985 *Rev. Mod. Phys.* **57** 827
[15] Finn R 1986 *Equilibrium Capillary Surfaces* (New York: Springer)
[16] Abramowitz M and Stegun I A (ed) 1972 *Handbook of Mathematical Functions* (New York: Dover)
[17] van Helden W G J, van der Geld C W M and Boot P G M 1995 *Int. J. Heat Mass Transfer* **38** 2075
[18] Marcout R, Zwilling J-F, Laherrere J M, Garrabos Y and Beysens D 1995 *Micrograv. Q.* **5** 162